



Review

Multistatic moving target detection in unknown coloured Gaussian interference



Bogomil Shtarkalev*, Bernard Mulgrew

Institute for Digital Communications, The University of Edinburgh, Edinburgh EH9 3JL, United Kingdom

ARTICLE INFO

Article history:

Received 8 December 2014

Received in revised form

8 March 2015

Accepted 1 April 2015

Available online 16 April 2015

Keywords:

Doppler radar

Multiple-input multiple-output (MIMO)

Target detection

Reduced-rank space–time adaptive processing (STAP)

Heterogeneous clutter

Gaussian approximation

ABSTRACT

One of the main interferers for a Doppler radar has always been the radar's own signal being reflected off the surroundings. This creates the problem of searching for a target in a coloured noise and interference environment. Traditional space–time adaptive processing (STAP) deals with the problem by using target-free training data to study this environment and build its characteristic covariance matrix. The maximum likelihood estimation detector (MLE) and its generalised counterpart (GMLED) are two reduced-rank STAP algorithms that eliminate the need for training data when mapping the statistics of the background interference. In this work the MLE and GMLED solutions to a multistatic scenario are derived. A hybrid multiple-input multiple-output (MIMO) system where each receiver is a coherent STAP radar has been employed. The focus of the work is the spatial diversity provided by the wide separation of the individual transmitter and receiver platforms. It is proven that this configuration does not affect the constant false alarm rate (CFAR) property of the bistatic radar case. A Gaussian approximation to the statistics of the multistatic algorithms is derived in order to provide a more in-depth analysis. The viability of the theoretical models and their approximations are tested against a numerical simulation.

© 2015 Elsevier B.V. All rights reserved.

1. Introduction

Multiple-input multiple-output (MIMO) radar with widely separated antennas has gained an increasing popularity over the past decade. The advantages of using multiple transmitters and receivers are numerous: higher accuracy of target localisation, higher detection rate under a certain false alarm probability, increased spatial and angular diversity, increased resolution [1–8]. All the benefits come at the cost of the additional elements in the system and the higher processing power that is required to obtain and utilise their observations. Apart from deliberate jamming techniques, ground clutter reflections are usually

the strongest interferers for Doppler radar. In the MIMO case this is likely to cause an even more significant problem due to the additional probing signals and their reflections present in the system. A well-known limitation of MIMO radar with fast-time orthogonal waveforms is the reduction of the region clear of sidelobes in the total ambiguity function [9,10]. This phenomenon has the potential to degrade the expected theoretical performance of a MIMO detector.

In this paper two single data set (SDS) [11–22,8] MIMO algorithms for target detection in coloured Gaussian clutter are presented. The strength of the algorithms is that they require neither prior knowledge of the spectral support or power of the background interference as in [18] nor access to secondary data as in [23–26] and thus can operate blindly in any environment. Moreover, in a heterogeneous environment there is no secondary data for

* Corresponding author. Tel.: +44 131 6505655.

E-mail addresses: b.shtarkalev@ed.ac.uk (B. Shtarkalev), b.mulgrew@ed.ac.uk (B. Mulgrew).

covariance estimation, thus leaving SDS detection as the only viable option.

Each receiver platform in the proposed algorithms operates coherently using the space–time adaptive processing (STAP) technique which boosts radar performance when dealing with ground clutter returns [27]. However, the main focus of this work is not on the coherent processing at each unit but rather on the cooperation between multiple widely spaced transmitters and STAP receivers as in [5]. Thus the maximum likelihood (ML) estimation and detection of a single target in such a multistatic scenario is derived where the whole radar network reaches a joint detection decision.

The proposed algorithms draw multiple low-rank snapshots from the observations of each STAP range gate. This greatly reduces the computational load associated with estimating and inverting the full STAP interference correlation matrix. Further rank-reduction of the algorithm can be achieved through the subspace projection methods proposed in [21,22].

The main contribution of this paper is the derivation of an approximate model for the statistics of the proposed MIMO detection algorithms. Extensive statistical analysis of the bistatic case has been derived and presented in [14,12,15]. As discussed in [23–26], the challenges associated with the theoretical analysis of mono/bistatic target detectors are compounded in multistatic widely spaced MIMO. Even when the individual bistatic paths (or channels) are mutually independent, it is unlikely that the corresponding general multistatic solutions exist in closed form [23–26,20]. In [24,26] a specific closed-form expression is provided for the pdf of a multistatic detector when no target is present in the system, and thus the multistatic probability of false alarm is derived. However, the corresponding derivation for the pdf and detection probability in the presence of targets is a problem of higher complexity that has not been solved. In this paper a methodology is proposed for deriving approximate expressions for probability of false alarm and detection for widely spaced MIMO systems. The methodology is illustrated in detail for the proposed SDS algorithms and could easily be extended to the theoretical analysis of other multistatic target detectors such as [23–26]. The key to obtaining the approximations is the application of the central limit theorem (CLT), or more precisely Lindeberg’s condition [28, p. 307], to the summation of bistatic detectors. This approximation enables the link between the radar operational parameters and the probabilities of detection and false alarm to be made.

The performance of the proposed detectors and the validity of the approximate statistical analysis are tested. It has been shown that the proposed detectors exhibit the highly desirable constant false alarm rate (CFAR) property. The two target detection algorithms have been simulated in a scenario involving a mixture of multiple transmit antennas and multiple receive phased arrays. A number of numerical tests have been performed that validate the approximate statistical analysis of the algorithms proposed in this paper. The advantages of the MIMO system with the increasing number of antennas in terms of detection probabilities are shown in the results.

Section 2 of this paper states the problem and assumptions of this work and provides a brief background on the most widely used target detection schemes currently available. Sections 3 and 4 provide the derivations of the two multistatic SDS radar detection algorithms proposed in this paper. Section 5 contains the statistical analysis of the detectors, the proposed Gaussian approximations. Section 6 contains the results of the numerical simulations and a discussion of these results. Section 7 presents the conclusions drawn from the work.

2. Problem formulation and background

This work focuses on widely separated (multistatic) radar detection, sometimes referred to as statistical MIMO radar. Consider a setup consisting of M transmit antennas and N receive arrays that probe an area for the presence of a moving target. Each array consists of P_T closely spaced elements that can perform coherent processing and STAP detection. However, as coherent processing is not the main focus of this work, each array is considered as a single unit, and the aim is to combine the detection capabilities of multiple widely separated such units. For simplicity and without loss of generality the receivers are assumed to be uniform linear arrays (ULA). Therefore each transmit–receive pair here forms a standard bistatic STAP system; this setup is often referred to as a single-input multiple-output (SIMO) coherent radar [29,30]. The term MIMO here is reserved for a multistatic setup (Fig. 1) and refers to non-coherent processing of a number of widely spaced STAP phased array receivers. Each of the ULA units collects K_T slow-time pulses per STAP range gate. A sliding window over the observation samples is used to produce K snapshots containing independent clutter observations, each one consisting of a total of P spatio-temporal samples (Fig. 2 top). The values of K and P can be arbitrary and chosen to suit a specific radar setup and clutter conditions, e.g. in clutter with heavy correlation, the sliding window can skip over samples and trade available data for estimation accuracy, the window can contain more than once slow-time pulse or only a part of a slow time pulse, etc.

Once obtained from the sliding window, the snapshots are vectorised by stacking their columns on top of each other and labelled as $\mathbf{x}_{m,n,k}$, $k=1\dots K$. The index $\{m,n\}$ signifies the path between the m th transmitter and the n th receiver. Throughout this work these different bistatic paths will be referred to as “channels.” Let the observation vectors be arranged as the columns of the observation matrix $\mathbf{X}_{m,n}$ (Fig. 2 bottom). If the complex amplitude of the returned signal in a channel is $\alpha_{m,n}$, the signal model for the observations in each individual bistatic STAP channel is the following:

$$\mathbf{X}_{m,n} = \alpha_{m,n} \mathbf{s}_{m,n} \mathbf{t}_{m,n}^T + \mathbf{N}_{m,n} \quad (1)$$

The superscript T indicates the transpose operator. The vectors $\mathbf{s}_{m,n}$ and $\mathbf{t}_{m,n}$ will be referred to as the spatial steering and the temporal steering vector respectively, and the matrix $\mathbf{N}_{m,n}$ is a combined term for the noise and interference in each channel. The spatial steering vector $\mathbf{s}_{m,n} \in \mathbb{C}^{P \times 1}$ is the template that the returned signal produces in each observation snapshot. It depends on the Doppler frequency of the

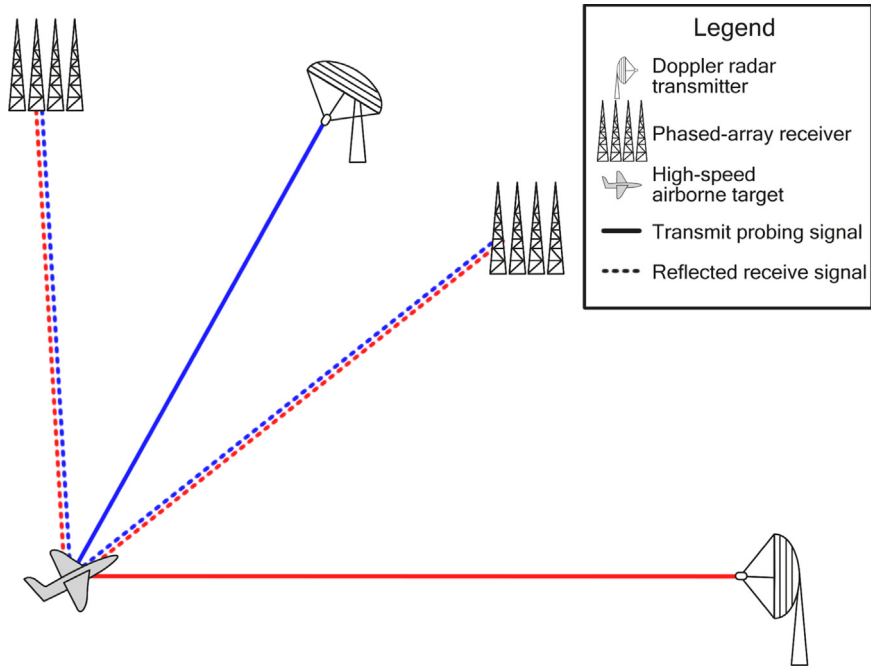


Fig. 1. Example of a 2-transmitter 2-receiver MIMO system.

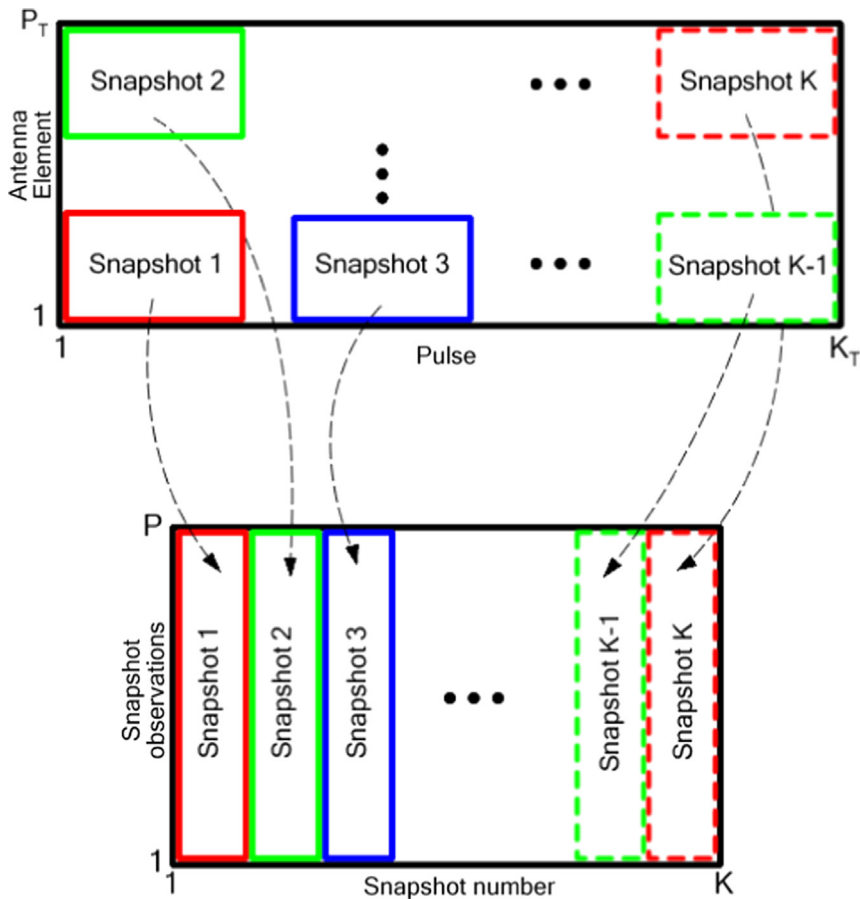


Fig. 2. Extracting snapshots containing iid clutter contributions with a sliding window over the STAP range gate (top) and vectorising them to produce the observation matrix $X_{m,n}$ (bottom).

incoming signal as well as the receiver ULA geometry and orientation. The temporal steering vector $\mathbf{t}_{m,n} \in \mathbb{C}^{K \times 1}$ indicates the complex phase relations between the K individual observation snapshots [12–16].

As already mentioned, the observation snapshots in (1) are obtained from windowing and rearranging the STAP samples of the cell under test (CUT) such that their clutter contributions are independent. This can be achieved through the choice of snapshots size P and snapshot number K parameters. It is likely that in reality some residual correlation between snapshot clutter will remain, but this will be neglected for the purpose of derivation in this work. Therefore the columns of the noise and interference matrix are assumed to be independent and identically distributed (iid) complex zero-mean Gaussian $\mathbf{n}_{m,n,k} \sim \mathcal{CN}_P(\mathbf{0}, \mathbf{C}_{m,n})$, each with a different autocorrelation matrix $\mathbf{C}_{m,n}$. The interference from channel to channel is also assumed to be independent. Because the snapshots size P is significantly smaller than the total number of observations in the CUT, the STAP signal model used here reduces the size of the correlation matrix that is estimated [31].

In addition to the interference, the pulses coming from the different transmitters in the system are also assumed to be nearly orthogonal to each other (low cross-correlation). A well-documented problem that arises from the simultaneous transmission of M ideal orthogonal waveforms at the same time and on the same bandwidth is the reduction of the clear region in the range-Doppler MIMO ambiguity function by a factor of M [9,10]. At the expense of additional bandwidth or delay, this problem can be alleviated by utilising time division multiple access (TDMA) or a frequency division multiple access (FDMA) methods for providing low cross-correlation between different transmit waveforms. As demonstrated in [32], such schemes result in negligible inter-channel interference between the different waveforms in the multistatic radar scenario. These additional resources are traded for the spatial diversity that MIMO radar provides in target detection. Finally, this paper assumes that the range-Doppler search space has been discretised (e.g. [33]), and the proposed detectors operate on each separate bin of the grid. Thus in the derivations that follow the Doppler frequencies $f_{m,n}^D$ and the array spatial response frequencies $f_{m,n}^{sp}$ are assumed to be known as they come from a specific range-Doppler CUT.

For the time being consider the signal model in (1) and only a single channel. Thus the index $\{m,n\}$ will be dropped for convenience for now. A bistatic STAP detection algorithm receives the observations \mathbf{X} and decides between two hypotheses for their origin

$$\begin{aligned} H_0: \mathbf{X} &= \mathbf{N} \\ H_1: \mathbf{X} &= \alpha \mathbf{s} \mathbf{t}^H + \mathbf{N} \end{aligned} \quad (2)$$

The optimum STAP pre-detection filter derived in [34] and normalised to exhibit the CFAR property is

$$\mathbf{w} = \frac{\mathbf{C}^{-1} \mathbf{s}}{\mathbf{s}^H \mathbf{C}^{-1} \mathbf{s}} \quad (3)$$

which is also known as the matched filter (MF). The superscript H indicates the Hermitian transpose. In a STAP system this filter is applied to the K individual observation snapshots, and the results are combined in the post-processing phase. A more efficient method is to combine

the observations in the pre-detection stage in the case of iid data. The amplitude and phase estimation (APES) filter presented in [35] proposes the STAP coherent sample mean vector for the observation data that can perform this task given the current observation model (1)

$$\mathbf{g} = \frac{1}{K} \mathbf{X} \mathbf{t}^* \quad (4)$$

It is assumed that the 2-norm of the temporal steering vector is $\|\mathbf{t}\|^2 = K$, and the superscript $*$ signifies the complex conjugate operator. Eq. (4) can also be seen as a narrow filtering operation that maximises the response to a certain space-time steering vector \mathbf{t} . The weighted output $\mathbf{w}^H \mathbf{g}$ is then used in a power threshold-comparison scheme in order to choose the more viable hypothesis from which the observations originated:

$$\frac{|\mathbf{s}^H \mathbf{C}^{-1} \mathbf{g}|^2}{\mathbf{s}^H \mathbf{C}^{-1} \mathbf{s}} \underset{H_0}{\overset{H_1}{\gtrless}} \gamma \quad (5)$$

Usually the covariance matrix \mathbf{C} of the noise and interference is not known. Traditional sample matrix inversion (SMI) detection algorithms have assumed the availability of a secondary data set \mathbf{Z} consisting of K_t target-free observation vectors of size $\mathbb{C}^{P \times 1}$ from which the sample covariance matrix estimate can be built:

$$\hat{\mathbf{C}} = \frac{1}{K_t} \mathbf{Z} \mathbf{Z}^H \quad (6)$$

Using (6) in (3) to replace the covariance matrix gives the adaptive matched filter (AMF) threshold detector [36]:

$$\frac{|\mathbf{s}^H \hat{\mathbf{C}}^{-1} \mathbf{g}|^2}{\mathbf{s}^H \hat{\mathbf{C}}^{-1} \mathbf{s}} \underset{H_0}{\overset{H_1}{\gtrless}} \gamma \quad (7)$$

Assuming that the covariance matrix \mathbf{C} is unknown from the start and minimising over it in the process, Kelly derived his generalised likelihood ratio test (GLRT) [37]:

$$\frac{|\mathbf{s}^H \hat{\mathbf{C}}^{-1} \mathbf{g}|^2}{\mathbf{s}^H \hat{\mathbf{C}}^{-1} \mathbf{s} (1 + \mathbf{g}^H \hat{\mathbf{C}}^{-1} \mathbf{g})} \underset{H_0}{\overset{H_1}{\gtrless}} \gamma \quad (8)$$

Because these algorithms rely on the availability of a secondary training data set, they are commonly known as two-data set (TDS) detectors [37,36]. In recent years SDS detection algorithms have gained an increasing popularity [11–22]. The reason for that is the fact that in a non-homogeneous or non-stationary environment the observation-free training data \mathbf{Z} required by traditional algorithms needs to be constantly re-estimated to match the changes in the background noise and interference. This creates a large data overhead, and given the ever-increasing air traffic nowadays, continuously obtaining target-free training observations may become difficult. With an SDS of observations \mathbf{X} , a system can construct a sample correlation estimate of the data in the same manner as (6):

$$\hat{\mathbf{R}} = \frac{1}{K} \mathbf{X} \mathbf{X}^H \quad (9)$$

Under H_0 the matrix (9) is an estimate to the central noise covariance matrix \mathbf{C} similar to (6), while under H_1 it is a non-central estimate of \mathbf{C} offset by the additional contribution $|\alpha|^2 \mathbf{s} \mathbf{s}^H$ from the target. The APES filter [35] shown in (10) can be used to derive an SDS estimate to the central noise

covariance matrix from (9)

$$\mathbf{w}^{APES} = \frac{\mathbf{Q}^{-1}\mathbf{s}}{\mathbf{s}^H\mathbf{Q}^{-1}\mathbf{s}} \quad (10)$$

$$\mathbf{Q} = \hat{\mathbf{R}} - \mathbf{g}\mathbf{g}^H \quad (11)$$

The sample covariance estimate (11) was utilised in the development of the maximum likelihood estimation detector (MLED) in [12], which is the SDS counterpart of the AMF detector:

$$\frac{|\mathbf{s}^H\mathbf{Q}^{-1}\mathbf{g}|^2}{\mathbf{s}^H\mathbf{Q}^{-1}\mathbf{s}} \underset{H_0}{\overset{H_1}{\gtrless}} \gamma \quad (12)$$

The generalised maximum likelihood estimation detector (GMLED) is also derived as the natural SDS counterpart to Kelly's GLRT [14, pp. 54–57, 12,15]:

$$\frac{|\mathbf{s}^H\mathbf{Q}^{-1}\mathbf{g}|^2}{\mathbf{s}^H\mathbf{Q}^{-1}\mathbf{s}(1 + \mathbf{g}^H\mathbf{Q}^{-1}\mathbf{g})} \underset{H_0}{\overset{H_1}{\gtrless}} \gamma \quad (13)$$

Both (12) and (13) are SDS threshold detection algorithms that are based on statistical modelling of the noise and interference through covariance estimation. A different algorithm that combines SDS and TDS detection is proposed in [16]. It exploits the benefits of both detection methods but still relies on forming an estimate to the statistics of the background noise and interference. A different approach of dealing with target detection in non-homogeneous environment is presented in [18]. It derives an SDS projection-based MIMO solution to the problem while avoiding the need to do any statistical analysis of the environment. The shortcoming of these methods is that prior information about the structure and spectral range of the clutter has to exist. The MLED and GMLED algorithms operate without any such prior knowledge. A comparison of the hybrid SMI, the TDS SMI, and the projections approaches has been conducted in [38]. The subspace approach has been further developed to incorporate the autoregressive clutter model from [17] in a MIMO projection-based scenario [20].

3. Multistatic maximum likelihood estimation detector

In this section the ML multistatic solution to the target detection problem in unknown coloured background noise is derived. The derivation is a more in-depth extension of [8]. The resulting detector is similar to the ones presented in [23,25] but does not use an independent training data set. The derivation mirrors that of its respective TDS counterpart and is included here for convenience. The setup described in Section 2 and the signal model (2) are adopted (note that the signal model is now channel-specific and applies to each channel). The channel-specific probability density function (pdf) of each observed data matrix $\mathbf{X}_{m,n}$ conditioned on the amplitude of the reflected probing signal $\alpha_{m,n}$ is given by [14, p. 121]

$$f(\mathbf{X}_{m,n}|\alpha_{m,n}) = \left(\frac{1}{\pi^p|\mathbf{C}_{m,n}|}\right)^K \text{etr}\{-\mathbf{C}_{m,n}^{-1}\mathbf{M}_{m,n}^\alpha\} \quad (14)$$

where $\mathbf{M}_{m,n}^\alpha = \sum_{k=1}^K (\mathbf{x}_{m,n,k} - \alpha_{m,n}\mathbf{s}_{m,n}\mathbf{t}_{m,n}(k))(\mathbf{x}_{m,n,k} - \alpha_{m,n}\mathbf{s}_{m,n}\mathbf{t}_{m,n}(k))^H$. It is assumed that the covariance matrices of the background interference $\mathbf{C}_{m,n}$ are known for the time being

in order to derive the optimal multistatic detector. Here the notation that $|\bullet|$ is the determinant, $\text{etr}(\bullet) = e^{\text{Tr}(\bullet)}$, and $\text{Tr}(\bullet)$ is the trace of the matrix (\bullet) has been adopted. In a MIMO system with sufficient separation between antennas, the background noise processes $\mathbf{N}_{m,n}$ are uncorrelated to one another. The joint pdf of the complete set of observations $\mathbb{X} = \{\mathbf{X}_{m,n}|m=1\dots M, n=1\dots N\}$ given the set of amplitudes $\mathbb{X} = \{\alpha_{m,n}|m=1\dots M, n=1\dots N\}$ can be represented by the product of the individual pdfs given in (14)

$$f(\mathbb{X}|\mathbb{X}) = \prod_{m,n} f(\mathbf{X}_{m,n}|\alpha_{m,n}) \\ = \left(\frac{1}{\pi^{MNP}\prod_{m,n}|\mathbf{C}_{m,n}|}\right)^K \text{etr}\left\{-\sum_{m,n} \mathbf{C}_{m,n}^{-1}\mathbf{M}_{m,n}^\alpha\right\} \quad (15)$$

Let $\mathbb{X} = \emptyset$ signify the case when every element of the set \mathbb{X} is equal to zero. Therefore, the joint pdf of the set of observation signals \mathbb{X} under the null hypothesis from (2) is given by

$$f_0(\mathbb{X}) = f(\mathbb{X}|\mathbb{X} = \emptyset) \\ = \left(\frac{1}{\pi^{MNP}\prod_{m,n}|\mathbf{C}_{m,n}|}\right)^K \text{etr}\left\{-\sum_{m,n} \mathbf{C}_{m,n}^{-1}\mathbf{M}_{m,n}^0\right\} \quad (16)$$

where $\mathbf{M}_{m,n}^0 = \sum_{k=1}^K \mathbf{x}_{m,n,k}\mathbf{x}_{m,n,k}^H$. Under hypothesis H_1 from (2), the joint pdf $f_1(\mathbb{X})$ is simply given by $f(\mathbb{X}|\alpha)$ from Eq. (15). To obtain the ML estimate of the unknown parameters in the set α , the logarithm of (15) is taken and then the partial derivative of the expression with respect to each unknown complex amplitude $\alpha_{m,n}$ individually is formed. The problem thus becomes linearly separable, and the solution is identical to the single channel case presented in [12]

$$\hat{\alpha}_{m,n} = \frac{\mathbf{s}_{m,n}^H\mathbf{C}_{m,n}^{-1}\mathbf{g}_{m,n}}{\mathbf{s}_{m,n}^H\mathbf{C}_{m,n}^{-1}\mathbf{s}_{m,n}} \quad (17)$$

Note that (17) is identical to the amplitude estimate of the APES filter derived in [35]. Forming the ML ratio of (15) and (16), the multistatic MLED threshold detector for a MIMO system is derived

$$\frac{\max_{\mathbb{X}} f_1}{f_0} = \frac{\text{etr}\{-\sum_{m,n} \mathbf{C}_{m,n}^{-1}\mathbf{M}_{m,n}^\alpha\}}{\text{etr}\{-\sum_{m,n} \mathbf{C}_{m,n}^{-1}\mathbf{M}_{m,n}^0\}} \\ = \text{etr}\left\{-\sum_{m,n} \mathbf{C}_{m,n}^{-1}(\mathbf{M}_{m,n}^\alpha - \mathbf{M}_{m,n}^0)\right\} \quad (18)$$

where $\mathbf{M}_{m,n}^\alpha = \sum_{k=1}^K (\mathbf{x}_{m,n,k} - \hat{\alpha}_{m,n}\mathbf{s}_{m,n}\mathbf{t}_{m,n}(k))(\mathbf{x}_{m,n,k} - \hat{\alpha}_{m,n}\mathbf{s}_{m,n}\mathbf{t}_{m,n}(k))^H$, with $\hat{\alpha}_{m,n}$ being the ML estimate given by (17).

The relationship between $\mathbf{M}_{m,n}^\alpha$ and $\mathbf{M}_{m,n}^0$ is derived in [14, p. 122] and is provided in Appendix A for convenience

$$\mathbf{M}_{m,n}^\alpha = \mathbf{M}_{m,n}^0 - K\mathbf{g}_{m,n}\mathbf{g}_{m,n}^H \\ + K(\mathbf{g}_{m,n} - \hat{\alpha}_{m,n}\mathbf{s}_{m,n})(\mathbf{g}_{m,n} - \hat{\alpha}_{m,n}\mathbf{s}_{m,n})^H \quad (19)$$

Plugging the relation (19) in (18), taking the logarithm of the expression, and using the identity $\mathbf{v}^H\mathbf{M}\mathbf{v} = \text{Tr}(\mathbf{M}\mathbf{v}\mathbf{v}^H)$ for an arbitrary vector \mathbf{v} and matrix \mathbf{M} , we obtain the ML multistatic threshold detector for the case when the covariance matrices of the background noise and interference $\mathbf{C}_{m,n}$ for

all different channels are known

$$T_{MF} = \sum_{m,n} \frac{|\mathbf{s}_{m,n}^H \mathbf{C}_{m,n}^{-1} \mathbf{g}_{m,n}|^2}{\mathbf{s}_{m,n}^H \mathbf{C}_{m,n}^{-1} \mathbf{s}_{m,n}} \stackrel{H_1}{\geq} \gamma \quad (20)$$

where γ is the decision threshold associated with the combined ML term from all channels. In the current problem, note that T_{MF} in (20) represents the multistatic matched filter-based detector which is an extension to the single-channel one described by (3) and (5). To obtain the multistatic MLED detector, the noise data covariance matrices $\mathbf{C}_{m,n}$ are replaced with their SDS APES estimates $\mathbf{Q}_{m,n}$ (11)

$$T_M = \sum_{m,n} \frac{|\mathbf{s}_{m,n}^H \mathbf{Q}_{m,n}^{-1} \mathbf{g}_{m,n}|^2}{\mathbf{s}_{m,n}^H \mathbf{Q}_{m,n}^{-1} \mathbf{s}_{m,n}} \stackrel{H_1}{\geq} \gamma \quad (21)$$

The ML SDS solution (21) to the MIMO case investigated in this work is a summation of the individual single-channel solutions (12) for each path $\{m, n\}$ in the system. The linear separability of the multistatic detector in the sum of the bistatic ones is in accordance with our prior assumption that the individual transmit-receive channels are independent.

4. Multistatic generalised maximum likelihood estimation detector

In this section the multistatic GMLED threshold test algorithm for SDS detection is derived. The derivation is a more in-depth extension of [8]. The resulting detector is similar to the multistatic generalised likelihood ratio test presented in [23–26] but does not require an independent training data set. The derivation is similar to that of its respective TDS counterpart and is included here for convenience. While in the derivation of the MLED the covariance matrices of the noise and interference signals $\mathbf{C}_{m,n}$ were assumed to be known, in the GMLED they are kept as unknown parameters from the start. The expression for the pdf of each individual observation signal set $\mathbf{X}_{m,n}$, now conditional on both the amplitude $\alpha_{m,n}$ and covariance matrix $\mathbf{C}_{m,n}$, is identical to the respective MLED case given by (14). Therefore, the joint pdf in the multistatic extension also remains the same as the one given in (15), this time conditional on the complete set of unknown covariance matrices $\mathcal{C}_v = \{\mathbf{C}_{m,n} | m = 1 \dots M, n = 1 \dots N\}$. This is also the expression that provides the relevant likelihood function under the H_1 hypothesis from (2). Under the alternative hypothesis, the likelihood function, now conditional on the parameter set \mathcal{C}_v , is the same as (16). If the logarithm of this expression is taken, the problem is once again linearly separable. Therefore, the maximum of (16) with respect to all $\mathbf{C}_{m,n}$ parameters is equivalent to maximising all the individual likelihoods in (14). As described in [14, p. 122, 12,15] this happens when the matrices $\mathbf{C}_{m,n}$ are replaced by their ML estimates $\hat{\mathbf{C}}_{m,n} = K^{-1} \mathbf{M}_{m,n}^0$, and the maximised likelihood function is thus

$$\max_{\mathcal{C}_v} f_0(\mathcal{X}) = \left(\frac{1}{(e\pi K)^{MNP} \prod_{m,n} |\mathbf{M}_{m,n}^0|} \right)^K \quad (22)$$

From the same source, the maximisation of the pdf under the alternative hypothesis occurs when $\mathbf{C}_{m,n}$ are replaced

by $\hat{\mathbf{C}}_{m,n} = K^{-1} \mathbf{M}_{m,n}^\alpha$, resulting in the following expression:

$$\max_{\mathcal{C}_v} f_1(\mathcal{X} | \mathcal{X}) = \left(\frac{1}{(e\pi K)^{MNP} \prod_{m,n} |\mathbf{M}_{m,n}^\alpha|} \right)^K \quad (23)$$

Noting that once again the conditioned likelihood (23) can be made linearly separable through taking the logarithm, the maximisation of the expression can be achieved when each of the individual terms $|\mathbf{M}_{m,n}^\alpha|$ is minimised with respect to $\alpha_{m,n}$. The solution is thus the same as the one provided in the single-channel GMLED derivation and is detailed in Appendix B:

$$\min_{\alpha_{m,n}} |\mathbf{M}_{m,n}^\alpha| = K^P |\mathbf{Q}_{m,n}| \left(1 + \mathbf{g}_{m,n}^H \mathbf{Q}_{m,n}^{-1} \mathbf{g}_{m,n} - \frac{|\mathbf{s}_{m,n}^H \mathbf{Q}_{m,n}^{-1} \mathbf{g}_{m,n}|^2}{\mathbf{s}_{m,n}^H \mathbf{Q}_{m,n}^{-1} \mathbf{s}_{m,n}} \right) \quad (24)$$

$$|\mathbf{M}_{m,n}^0| = K^P |\mathbf{Q}_{m,n}| (1 + \mathbf{g}_{m,n}^H \mathbf{Q}_{m,n}^{-1} \mathbf{g}_{m,n}) \quad (25)$$

Forming the ratio of the maximised likelihoods (23) and (22), the multistatic threshold detector expression can be obtained

$$\frac{\max_{\mathcal{C}_v} f_1}{\max_{\mathcal{C}_v} f_0} = \left(\frac{\prod_{m,n} |\mathbf{M}_{m,n}^0|}{\prod_{m,n} \min_{\alpha_{m,n}} |\mathbf{M}_{m,n}^\alpha|} \right)^K \quad (26)$$

Plugging in the relevant expressions for the determinants (24) and (25) into (26) and forming the K th root of the likelihood ratio, the expression for the multistatic GMLED is obtained

$$T_G = \prod_{m,n} \frac{1 + \mathbf{g}_{m,n}^H \mathbf{Q}_{m,n}^{-1} \mathbf{g}_{m,n}}{1 + \mathbf{g}_{m,n}^H \mathbf{Q}_{m,n}^{-1} \mathbf{g}_{m,n} - \frac{|\mathbf{s}_{m,n}^H \mathbf{Q}_{m,n}^{-1} \mathbf{g}_{m,n}|^2}{\mathbf{s}_{m,n}^H \mathbf{Q}_{m,n}^{-1} \mathbf{s}_{m,n}}} \stackrel{H_1}{\geq} \nu \quad (27)$$

where ν is the decision threshold associated with the combined ML threshold detector. The multistatic GMLED (27) is a product of the bistatic solutions (13) for each path $\{m, n\}$ in the system expressed in their original form.

5. Analysis

This section provides a statistical analysis of the derived multistatic versions of the MLED and GMLED algorithms. To derive an expression for the probability of false alarm P_{fa} and the probability of detection P_d , the CLT is employed to obtain a Gaussian approximation to both threshold detectors' pdfs for a large number $M \times N$ of transmit-receive pairs.

5.1. Statistical properties of the multistatic MLED

The statistical properties of the bistatic MLED detector are described in [14, pp. 63–65, 12,15]. The detection test for a single bistatic channel shown in (12) is thus equivalent to

$$\frac{\zeta_{m,n}}{L \eta_{m,n}} \stackrel{H_1}{\geq} \gamma_{m,n} \quad (28)$$

where $L = K - P$. The random variables $\zeta_{m,n}$ and $\eta_{m,n}$ are mutually independent. The random variable $\eta_{m,n}$ follows the type I beta distribution with $L + 1$ and $P - 1$ degrees of

freedom. The random variable $\zeta_{m,n}$ is distributed according to the non-central F distribution with 2 and $2L$ degrees of freedom and a non-centrality parameter $\lambda_{m,n}$ given by

$$\lambda_{m,n} = 2KP\eta_{m,n}\rho_{m,n} \quad (29)$$

The signal-to-noise ratio (SNR) $\rho_{m,n}$ for each antenna element and pulse in a single channel is derived in [14, p. 17, 12,15]

$$\rho_{m,n} = \frac{1}{P} \left| \alpha_{m,n} \right|^2 \mathbf{s}_{m,n}^H \mathbf{C}_{m,n}^{-1} \mathbf{s}_{m,n} \quad (30)$$

In the case where no target is present in the set of observations $\mathbf{X}_{m,n}$, the non-centrality parameter $\lambda_{m,n}$ becomes zero, and the random variable $\zeta_{m,n}$ has a central F -distribution with 2 and $2L$ degrees of freedom. Using (21), the multistatic MLED detection test statistics are distributed as

$$\sum_{m,n} \frac{\zeta_{m,n}}{L\eta_{m,n}} \underset{H_0}{\overset{H_1}{\gtrless}} \gamma \quad (31)$$

The test statistics consists of a sum of random terms shown in [12] to be independent of the underlying noise and interference. Therefore, the multistatic MLED is also independent of the statistics of the noise, preserving the CFAR property in the MIMO extension of the algorithm. Due to the complex nature of the random variables involved, obtaining a closed form expression for the pdf of the multistatic MLED detector would be difficult and impractical. Similar conclusions have been reached in both [23,25] where analogical TDS MIMO algorithms for target detection have been proposed. The bistatic approach to the test statistics in (31) is to assume that the random variable η is known, which results in the detection variable having the non-central F -distribution. This pdf can then be integrated to obtain an expression for the probability of detection and the probability of false alarm. In the multistatic case assuming that all variables $\eta_{m,n}$ are known results in the detection variable being a sum of $M \times N$ independent non-identically distributed non-central F -distributed random variables. The pdf of such random variable is not trivial to obtain which makes analysis of the proposed multistatic algorithm difficult. However, if the sum in (31) consists of enough terms, it can be approximated by a normal distribution. This enables the derivation of approximate expressions for the probability of false alarm $P_{Mf}(\gamma)$ and the probability of detection $P_{Md}(\gamma)$ for a given detection threshold γ . The approach and solution can be easily extended to existing TDS detectors [23,25] by using the appropriate parameters and degrees of freedom for those algorithms.

5.2. Gaussian approximation of the multistatic MLED

The multistatic MLED threshold detector consists of a sum of $M \times N$ independent random terms as shown in (31). The CLT dictates that the statistics of the decision variable can be closely approximated by a Gaussian distribution, i.e. $T_M \sim \mathcal{N}(\mu_M, \sigma_M^2)$, provided that $M \times N$ is sufficiently large. Because the terms are not identically distributed, Lindeberg's condition has to be satisfied which is shown in Appendix C. The mean μ_M and variance σ_M^2 are

given by the sum of the means and variances of the individual terms in the detector

$$\mu_M = \sum_{m,n} \mu_{M(m,n)} \quad (32)$$

$$\sigma_M^2 = \sum_{m,n} \sigma_{M(m,n)}^2 \quad (33)$$

$$\mu_{M(m,n)} = E \left[\frac{\zeta_{m,n}}{L\eta_{m,n}} \right] \quad (34)$$

$$\sigma_{M(m,n)}^2 = \text{var} \left(\frac{\zeta_{m,n}}{L\eta_{m,n}} \right) \quad (35)$$

Here $E[\bullet]$ signifies the expectation and $\text{var}(\bullet)$ the variance of the random variable or vector \bullet . Because the random variables $\zeta_{m,n}$ and $\eta_{m,n}$ are independent, the central moments of their ratios factorise in the following manner [39]:

$$\mu_{M(m,n)} = \frac{1}{L} E[\zeta_{m,n}] E \left[\frac{1}{\eta_{m,n}} \right] \quad (36)$$

$$\sigma_{M(m,n)}^2 = \frac{1}{L^2} E[\zeta_{m,n}^2] E \left[\left(\frac{1}{\eta_{m,n}} \right)^2 \right] - \frac{1}{L^2} E[\zeta_{m,n}]^2 E \left[\frac{1}{\eta_{m,n}} \right]^2 \quad (37)$$

Provided that $L > 2$, which can be ensured by collecting enough slow-time samples K at each node, the first two central moments of the F -distributed random variable $\zeta_{m,n}$ are given in statistics literature [40]

$$E[\zeta_{m,n}] = \frac{L2 + \lambda_{m,n}}{2L - 1} \quad (38)$$

$$\text{var}(\zeta_{m,n}) = \frac{L^2(2 + \lambda_{m,n})^2 + 4(1 + \lambda_{m,n})(L - 1)}{4(L - 1)^2(L - 2)} \quad (39)$$

The first two central moments of $\eta_{m,n}^{-1}$ are obtained by solving the expectation integral of the reciprocal beta-distributed random variable with $L + 1$ and $P - 1$ degrees of freedom

$$E \left[\frac{1}{\eta_{m,n}} \right] = \frac{K - 1}{L} \quad (40)$$

$$\text{var} \left(\frac{1}{\eta_{m,n}} \right) = \frac{(K - 1)(P - 1)}{L^2(L - 1)} \quad (41)$$

Using the fact that $E[\bullet^2] = \text{var}(\bullet) + E[\bullet]^2$, (38)–(41) can be plugged in (34) and (35) to obtain an expression for the mean and variance of the random variable that signifies the bistatic MLED threshold detector

$$\mu_{M(m,n)} = \frac{K - 1}{2L} \frac{2 + \tilde{\lambda}_{m,n}}{L - 1} \quad (42)$$

$$\sigma_{M(m,n)}^2 = \frac{(K - 1)(K + P - 2)(2 + \tilde{\lambda}_{m,n})^2}{4L^2(L - 1)^2(L - 2)} + \frac{(K - 1)(K - 2)(1 + \tilde{\lambda}_{m,n})}{L(L - 1)^2(L - 2)} \quad (43)$$

where it has been accounted for the fact that $\lambda_{m,n}$ is a random variable dependent on $\eta_{m,n}$ by replacing it with its expected value $\tilde{\lambda}_{m,n}$ given by

$$\begin{aligned} \tilde{\lambda}_{m,n} &= E[2KP\rho_{m,n}\eta_{m,n}] \\ &= 2P(L + 1)\rho_{m,n} \end{aligned} \quad (44)$$

It should be noted that (44) is an additional approximation that is performed for convenience. The CLT holds without replacing the variables $\lambda_{m,n}$ with their first order estimates proposed here. Without this approximation however both the mean (34) and the variance (35) of the normal distribution used to describe the detector statistics are random variables. Integrating over all the $\eta_{m,n}$ variables in the Gaussian pdf is the approach that would be taken in the bistatic detector case, but once again in the multistatic version this is impractical and has no trivial solution which justifies the usage of (44). To obtain the probability of false alarm for a given threshold γ , it is noted that in the absence of target the multistatic MLED threshold detector is approximately distributed as $\mathcal{N}(\mu_{M0}, \sigma_{M0}^2)$ where

$$\mu_{M0} = \sum_{m,n} \mu_{m,n}(\tilde{\lambda}_{m,n} = 0) \quad (45)$$

$$\sigma_{M0}^2 = \sum_{m,n} \sigma_{m,n}^2(\tilde{\lambda}_{m,n} = 0) \quad (46)$$

Therefore the false alarm probability P_f is approximately

$$P_{Mf}(\gamma) = Q\left(\frac{\gamma - \mu_{M0}}{\sigma_{M0}}\right) \quad (47)$$

where $Q(x)$ is the Q-function associated with the tail probability $\Pr[X > x]$ of the standard normal distribution. The probability of detection is obtained in the case where a target is present in the observations. The multistatic MLED detector variable is then approximately distributed as $\mathcal{N}(\mu_{M1}, \sigma_{M1}^2)$, where μ_{M1} and σ_{M1}^2 are the same sums as (32) and (33) respectively with the $\tilde{\lambda}_{m,n}$ parameters given by (44). Thus

$$P_{Md}(\gamma) = Q\left(\frac{\gamma - \mu_{M1}}{\sigma_{M1}}\right) \quad (48)$$

Note that the Gaussian approximation to the multistatic MLED proposed here can be easily extended to the multistatic AMF proposed in [23,25]. The approach closely follows the one presented in this work and is thus not provided.

5.3. Statistical properties of the multistatic GMLED

The analysis of the GMLED in [14, pp. 54–63, 12,15] has been performed for the threshold detector expressed in the form given in (13). The multistatic expression (27) requires the return to the original GMLED likelihood ratio expressed as

$$T_{G(m,n)} = \frac{1}{1 - \frac{|\mathbf{s}_{m,n}^H \mathbf{Q}_{m,n}^{-1} \mathbf{g}_{m,n}|^2}{\mathbf{s}_{m,n}^H \mathbf{Q}_{m,n}^{-1} \mathbf{s}_{m,n} (1 + \mathbf{g}_{m,n}^H \mathbf{Q}_{m,n}^{-1} \mathbf{g}_{m,n})}} \underset{H_0}{\underset{H_1}{\gtrless}} \nu_{m,n} \quad (49)$$

where $\nu_{m,n} = (1 - \gamma_{m,n})^{-1}$ is the relation between the transformations of the threshold in the bistatic case. The statistical distribution of (49) is thus equivalent to

$$\frac{\zeta_{m,n}}{L} + 1 \underset{H_0}{\underset{H_1}{\gtrless}} \nu_{m,n} \quad (50)$$

where $\zeta_{m,n}$ is the same random variable from the MLED statistics. The multistatic GMLED threshold detector in

(27) is therefore distributed as

$$\prod_{m,n} \left(\frac{\zeta_{m,n}}{L} + 1 \right) \underset{H_0}{\underset{H_1}{\gtrless}} \nu \quad (51)$$

The test statistics thus consist of a product of random terms that were shown in [14, p. 61, 12,15] to be independent of the underlying noise and clutter distributions. Therefore, the multistatic GMLED threshold detector is, in turn, independent of the statistics of the noise, preserving the CFAR property in the MIMO extension of the algorithm. Similar to the multistatic MLED detector, its generalised extension is difficult to analyse in the statistical sense. In [24,26] statistical analysis of the multistatic TDS detector derived from Kelly's GLRT is provided. However, closed-form expressions for the detection variable pdf exist only for the case when no target is present (hypothesis H_0 here), and thus only the probability of false alarm is derived. A general closed-form expression for the multistatic detector's pdf has not been reached. Therefore, in the next section an approximation to the statistics of the detector in (51) is provided given that a large number of terms take part in the product. As a result it is possible to derive approximate expressions for the probability of false alarm $P_{Cf}(\nu)$ and the probability of detection $P_{Cd}(\nu)$ for a given detection threshold ν . The approach and solution can be easily extended to existing TDS detectors [23–26] by using the appropriate parameters and degrees of freedom for those algorithms.

5.4. Log-normal approximation of the multistatic GMLED

The multistatic GMLED threshold detector consists of a product of $M \times N$ random terms as shown in (51). It would be convenient to take the logarithm of this product to transform it into a sum of random variables

$$\log T_G = \sum_{m,n} \log T_{G(m,n)} \underset{H_0}{\underset{H_1}{\gtrless}} \log \nu \quad (52)$$

The CLT dictates that the statistics of the logarithm of the decision variable given in (52) can be closely approximated by a Gaussian distribution, i.e. $\log T_G \sim \mathcal{N}(\mu_G, \sigma_G^2)$, provided that the number of signal paths $M \times N$ in the system is sufficiently large. Once again the random variables in the sum are not identically distributed so a proof of the validity of Lindeberg's condition for the detector is given in Appendix D. Because the exponential of a normally distributed random variable follows the log-normal distribution with the same parameters, it can be concluded that in a large network $T_G \sim \text{lnN}(\mu_G, \sigma_G^2)$. To obtain expressions for the parameters of this distribution, the first two moments of the multistatic GMLED random variable have to be obtained. The expectation of the individual terms in the product (27) can be obtained from (50) by using the expectation of an F -distributed random variable given in (38)

$$E[T_{G(m,n)}] = \frac{2L + \lambda_{m,n}}{2(L-1)} \quad (53)$$

Because it is assumed that the random variables coming from the different channels $T_{G(m,n)}$ are independent, the expectation of their product factorises into a product of

their expectations. Therefore, the first moment of the multistatic GMLED random variable is given by

$$E[T_G] = \prod_{m,n} \frac{2L + \lambda_{m,n}}{2(L-1)} \quad (54)$$

The second moment of the individual product terms $T_{G(m,n)}$ is obtained from the variance of the F -distributed random variable given in (39) and the derived first moment (53).

$$E[T_{G(m,n)}^2] = \frac{(\lambda_{m,n} + 2L)^2 - 4L}{4(L-1)(L-2)} \quad (55)$$

The second moment of the multistatic GMLED detection variable is the product of the second moments of the statistically independent individual terms $T_{G(m,n)}$

$$E[T_G^2] = \prod_{m,n} \frac{(\lambda_{m,n} + 2L)^2 - 4L}{4(L-1)(L-2)} \quad (56)$$

From statistics literature, the first and second moments of a random variable T_G following the log-normal distribution with parameters μ_G and σ_G^2 are given by

$$E[T_G] = e^{\mu_G + \sigma_G^2/2} \quad (57)$$

$$E[T_G^2] = e^{2\mu_G + 2\sigma_G^2} \quad (58)$$

The derived expectations (54) and (56) and the parametric expressions (57) and (58) form a system of two equations. Solving the system for the parameters of the approximating distribution μ_G and σ_G^2 results in

$$\mu_G = \frac{1}{2} \sum_{m,n} \log \left(\frac{(\tilde{\lambda}_{m,n} + 2L)^4 (L-2)}{4((\tilde{\lambda}_{m,n} + 2L)^2 - 4L)(L-1)^3} \right) \quad (59)$$

$$\sigma_G^2 = \sum_{m,n} \log \left(\frac{((\tilde{\lambda}_{m,n} + 2L)^2 - 4L)(L-1)}{(\tilde{\lambda}_{m,n} + 2L)^2 (L-2)} \right) \quad (60)$$

where once again the random variables $\lambda_{m,n}$ have been replaced with their expected values $\tilde{\lambda}_{m,n}$ given by (44). In the absence of target the threshold detector is distributed as $\ln \mathcal{N}(\mu_{G0}, \sigma_{G0}^2)$ where μ_{G0} and σ_{G0}^2 no longer need to be approximated. Their exact values can be computed due to the fact that for $\lambda_{m,n} = 0$ the non-central F distribution becomes a central F distribution with 2 and $2L$ degrees of freedom, and the pdf of the distribution simplifies to

$$f_{2,2L}(x) = \frac{1}{\left(1 + \frac{x}{L}\right)^{L+1}} \quad (61)$$

Thus the integral expression for the first and second central moments of the logarithm of the bistatic GMLED random variable becomes solvable and yields the following results for the multistatic one which are no longer approximations:

$$\mu_{G0} = \frac{MN}{L} \quad (62)$$

$$\sigma_{G0}^2 = \frac{MN}{L^2} \quad (63)$$

The probability of false alarm for a certain threshold ν is

$$P_{Gf}(\nu) = Q \left(\frac{\log \nu - \mu_{G0}}{\sigma_{G0}} \right) \quad (64)$$

When a target is present the detector statistics are distributed as $\ln \mathcal{N}(\mu_{G1}, \sigma_{G1}^2)$ where μ_{G1} and σ_{G1}^2 are given by (59) and (60) respectively. The probability of detection is thus

$$P_{Gd}(\nu) = Q \left(\frac{\log \nu - \mu_{G1}}{\sigma_{G1}} \right) \quad (65)$$

Note that the log-normal approximation to the multistatic GMLED proposed here can be easily extended to the multistatic GLRT proposed in [23–26]. The approach closely follows the one presented in this work and is thus not provided.

6. Simulations

The multistatic MLED and GMLED algorithms were simulated in order to show the viability of the theoretical models and approximations presented in this work. Three approaches to the performance analysis of the models have been used. The first approach is a numerical Monte Carlo simulation of the proposed algorithms in (21) and (27). The results from these runs are labelled as “simulated” in the presented figures. The second simulation approach that is undertaken is based on the theoretical analysis of the multistatic MLED and GMLED algorithms. A closed-form expression for the test statistics of the detectors was never obtained. Therefore, the theoretical simulation results have been obtained through drawing samples from the random variables (31) and (51) presented in the analysis of the two algorithms. Instead of doing a Monte Carlo simulation to generate the $\lambda_{m,n}$ random variables, the first order approximation in (44) was used. These sets of results are labelled as “theoretical” in the provided figures. The third implemented approach aims to show the viability of the normal and log-normal approximations developed in this paper. These results are labelled as “approximation” on the figures.

The operational parameters of the transmitted pilots are the same as the ones in [18]. A pulse repetition frequency of 500 Hz, carrier frequency of 1 GHz, and target velocity of 30 m/s are set. It is also assumed that the direction of movement of the target is known which means that the exact velocity $\mathbf{v} = [v_x, v_y]^T$ in the (x, y) -direction is known given 2-dimensional motion. A number of experiments have been done with a smaller setup of $M = N = 10$ transmitters and receivers and a larger one of $M = N = 20$. The geometry of the MIMO setup consists of random placement of transmitters and receive ULAs. The amplitudes of the returned pilots $\alpha_{m,n}$ are also chosen at random from a complex normal distribution $\mathcal{CN}(0, 1)$. The exact formula for obtaining the Doppler frequencies of the returned pilots in the sense of MIMO radar can be found in [18,41]. The receiver ULA has $P_T = 5$ elements that collect $K_T = 40$ and $K_T = 120$ pulses per CPI. These slow-time observations have been rearranged into data snapshots of size $P = 10$, where the number of snapshots is $K = 20$ and $K = 60$. To generate the clutter in each channel, the general clutter model presented in [31] has been used. The spectrum of the clutter exhibits low-pass behaviour and is also roughly shaped in accordance to the realistic model discussed in [42, pp. 293–322]. The simulations consist of 10^6 Monte Carlo runs of each system for different SNR

values and depict the average probability of detection for each case when the probability of false alarm has been fixed to 2×10^{-2} . The SNR follows the definition in (30) and is assumed to be the same for all channels in the system.

Fig. 3 shows the obtained results for the smaller network of 10 transmitters and 10 receivers and $K=20$ snapshots. As expected, the GMLED algorithm performs slightly better than the MLED one for a small K , exhibiting the same probability of detection at approximately 1 dB less SNR. The results show that the simulated detector curves based on (21) and (27) match the theoretical models describing their statistics shown in (31) and (51) respectively. Moreover, the fact that the approximation to the $\lambda_{m,n}$ variables was used in the theoretical curves proves the viability and justifies the usage of (44). The Gaussian approximations to the multistatic detectors given in (47), (48), (64) and (65) are also close to the simulated and theoretical curves. The small offset comes from the fact that approximation based on the first two moments of the multistatic MLED and GMLED threshold detector random variables is performed. Moreover, the convergence of sums of non-identically distributed random variables to the CLT is usually slower than the iid counterparts. As it will be show, the approximations become much better as the number of transmitters and receivers in the system increases.

Fig. 4 shows the simulation results under the same conditions as Fig. 3 except the number of snapshots is now $K=60$. It can be seen that both the multistatic MLED and GMLED are significantly affected by the temporal frame size, having the same detection rate at approximately 6 dB lower SNR value. This can be explained by the improvement of the SDS covariance matrix estimate (11) through the addition of more data samples. It should be noted that as the temporary frame size increases, the multistatic MLED and GMLED algorithms' performance becomes almost identical. This is evident in the simulations as well and reflects the behaviour of the MLED and GMLED bistatic algorithms presented in [12,14,15].

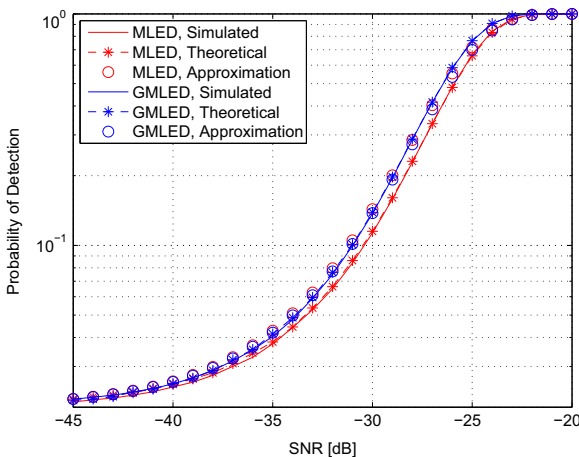


Fig. 3. Probability of detection vs SNR of the multistatic MLED and GMLED detectors for $P_{Mf} = 2 \times 10^{-2}$ and $P_{Cf} = 2 \times 10^{-2}$, $K=20$, $M=N=10$.

Fig. 5 aims to simulate the performance of a larger radar network. The number of transmitters and receivers doubles. Compared to Fig. 4, the curve of the probability of detection shifts by a further 3 dB to the left. This reflects the improvement in the performance of the multistatic MLED and GMLED detectors due to the increased spatial diversity in the system. The accuracies of the proposed Gaussian and log-normal approximations to the multistatic MLED and GMLED respectively are also greatly enhanced. This is because the number of terms in the summations (31) and (52) increases which, according to the CLT, brings the distribution of the sums closer to the Gaussian curve. In a hypothetical radar network of infinite size this approximation will become exact.

Fig. 6 presents an investigation into the relative approximation error of the detection probability provided by the Gaussian models proposed in this work. As expected, the approximation is poor for a small number of channels in the multistatic system. This is due to the fact that there are not enough random variables coming from the different

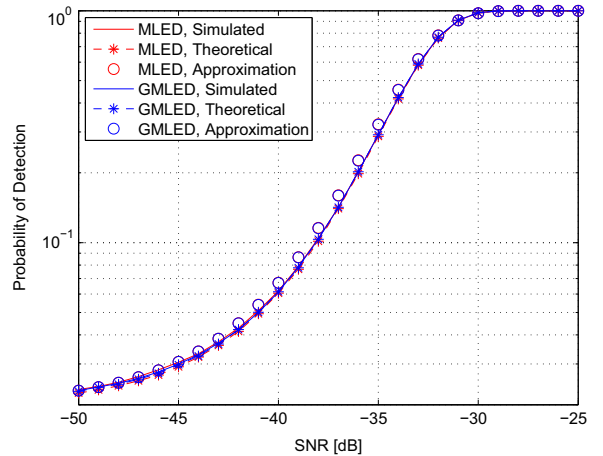


Fig. 4. Probability of detection vs SNR of the multistatic MLED and GMLED detectors for $P_{Mf} = 2 \times 10^{-2}$ and $P_{Cf} = 2 \times 10^{-2}$, $K=60$, $M=N=10$.

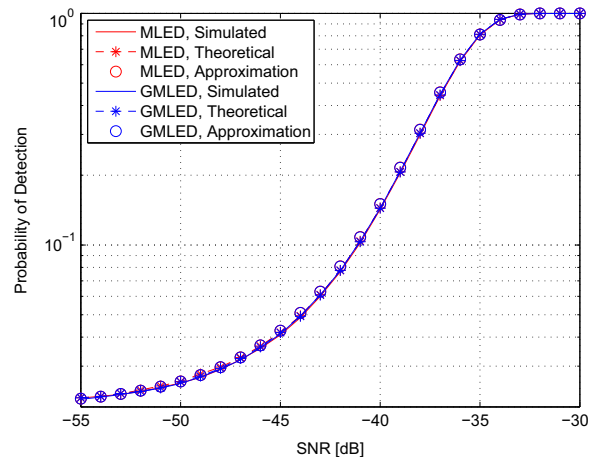


Fig. 5. Probability of detection vs SNR of the multistatic MLED and GMLED detectors for $P_{Mf} = 2 \times 10^{-2}$ and $P_{Cf} = 2 \times 10^{-2}$, $K=60$, $M=N=20$.

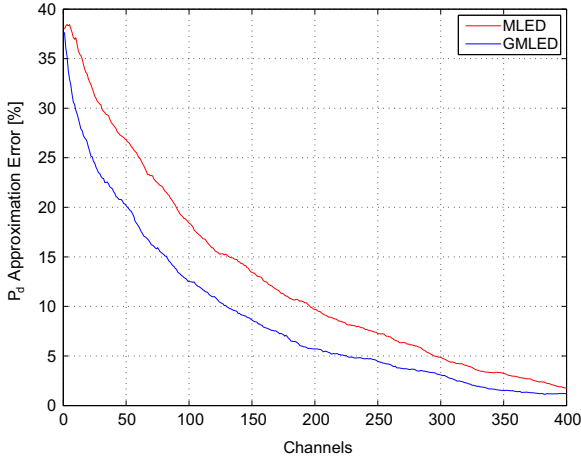


Fig. 6. Relative error of estimation of P_{Md} and P_{Gd} for $P_{Mf} = 2 \times 10^{-2}$ and $P_{Gf} = 2 \times 10^{-2}$, $K=20$.

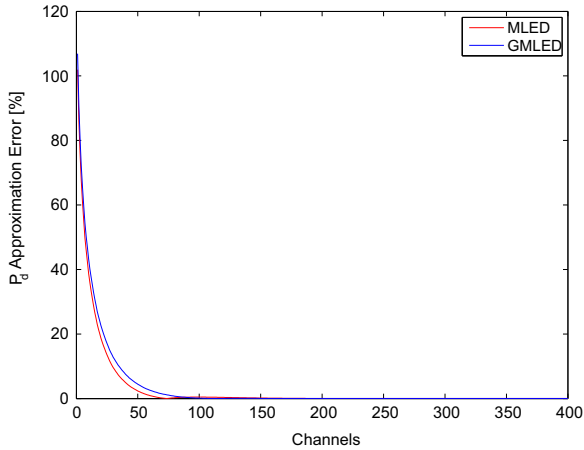


Fig. 7. Relative error of estimation of P_{Md} and P_{Gd} for $P_{Mf} = 2 \times 10^{-2}$ and $P_{Gf} = 2 \times 10^{-2}$, $K=60$.

channels to provide reliable convergence of the CLT. As more channels are added to the system, the approximation continues to get asymptotically closer to the real value of the detection probability.

Another factor that influences the approximation error is the number of iid snapshots in the system K . Fig. 7 shows the relative approximation error of the detection probability as a function of the number of channels for $K=60$ snapshots. It is clear that the convergence of the combination of bistatic random variables to the CLT is much quicker. The reason for this phenomenon is found in the higher moments of the underlying central and non-central F distributions present in the statistical analysis of the MLED and GMLED algorithms. As K increases, the higher moments of these distributions get smaller [40]. Thus the distributions become more and more Gaussian-like, which inherently speeds up the convergence rate to an actual bell-shaped curve after multiple convolutions.

7. Conclusion

This work proposes two SDS multistatic STAP algorithms for the detection of signals of known template in coloured Gaussian interference. The performance of the multistatic algorithms in a MIMO radar target detection scheme has been analysed. It has been shown that the algorithms exhibit the CFAR property. In order to analyse the system, simplified Gaussian approximation models for the statistics of the detectors have been proposed. Through these models the theoretical probabilities of detection and false alarm have been derived. The validity of the theoretical models as well as the simplified Gaussian approximations has been verified through numerical simulations. The performance gains of the multistatic detectors over their bistatic counterparts have been shown.

Acknowledgements

This work was supported by the Institute for Digital Communications at the University of Edinburgh, Selex ES and EPSRC (EP/J015180/1).

Appendix A. Detailed derivation of Eq. (19)

This appendix contains a detailed description of the steps required to obtain Eq. (19). The steps are originally found in [14, p. 122] and are provided here for convenience. All references to the index $\{m, n\}$ indicating the path between the m th transmitter and the n th receiver are omitted in this proof. The matrices \mathbf{M}^0 and $\mathbf{M}^{\hat{\alpha}}$ introduced earlier are defined as

$$\mathbf{M}^0 = \sum_{k=1}^K \mathbf{x}_k \mathbf{x}_k^H \quad (\text{A.1})$$

$$\mathbf{M}^{\hat{\alpha}} = \sum_{k=1}^K (\mathbf{x}_k - \hat{\alpha} \mathbf{st}(k)) (\mathbf{x}_k - \hat{\alpha} \mathbf{st}(k))^H \quad (\text{A.2})$$

Expanding (A.2), the connection with (A.1) can be made

$$\begin{aligned} \mathbf{M}^{\hat{\alpha}} &= \sum_{k=1}^K \mathbf{x}_k \mathbf{x}_k^H - \sum_{k=1}^K \hat{\alpha}^* \mathbf{x}_k \mathbf{t}^*(k) \mathbf{s}^H \\ &\quad - \sum_{k=1}^K \hat{\alpha} \mathbf{st}^T(k) \mathbf{x}_k^H + \sum_{k=1}^K |\hat{\alpha}|^2 |\mathbf{t}(k)|^2 \mathbf{ss}^H \\ &= \mathbf{M}^0 - K \hat{\alpha}^* \mathbf{gs}^H - K \hat{\alpha} \mathbf{sg}^H + K |\hat{\alpha}|^2 \mathbf{ss}^H \end{aligned} \quad (\text{A.3})$$

where the substitution for \mathbf{g} from (4) has been made, and the fact that in this work $|\mathbf{t}|^2 = K$ has been used. Adding and subtracting the term $K \mathbf{gg}^H$ to (A.3) and grouping the factors, the desired results in (19) are obtained. The factor K comes from the normalisation of the power of the temporary steering vector which is arbitrary. In some works it is set to unity and is therefore omitted. In this work the factor is simply included into the threshold γ of the target detector.

Appendix B. Detailed derivation of Eqs. (24) and (25)

This appendix contains a detailed description of the steps required to obtain Eqs. (24) and (25). Some of the steps are originally found in [14, p. 123] and are provided here for convenience. All references to the index $\{m, n\}$ indicating the path between the m th transmitter and the n th receiver are omitted in this proof.

Note that (19) can be written in terms of the SDS covariance estimation matrix \mathbf{Q} that directly follows from its definition in (11) and the fact that $\hat{\mathbf{R}}$ is defined as a scaled version of \mathbf{M}^0

$$\mathbf{M}^\alpha = K\mathbf{Q} + K(\mathbf{g} - \alpha\mathbf{s})(\mathbf{g} - \alpha\mathbf{s})^H \quad (\text{B.1})$$

Using the generalisation of Sylvester's identity for matrix determinants [43] it can be shown that, following from (B.1)

$$|\mathbf{M}^\alpha| = K^P |\mathbf{Q}| (1 + (\mathbf{g} - \alpha\mathbf{s})^H \mathbf{Q}^{-1} (\mathbf{g} - \alpha\mathbf{s})) \quad (\text{B.2})$$

Eq. (24) is obtained after minimising (B.2) with respect to the unknown return amplitude α by solving the partial derivative

$$\begin{aligned} \frac{\partial}{\partial \alpha^*} |\mathbf{M}^\alpha| &= \frac{\partial}{\partial \alpha^*} K^P |\mathbf{Q}| \left(1 + (\mathbf{g} - \alpha\mathbf{s})^H \mathbf{Q}^{-1} (\mathbf{g} - \alpha\mathbf{s}) \right) \\ &= -K^P |\mathbf{Q}| \mathbf{s}^H \mathbf{Q}^{-1} (\mathbf{g} - \alpha\mathbf{s}) \\ &= \alpha K^P |\mathbf{Q}| \mathbf{s}^H \mathbf{Q}^{-1} \mathbf{s} - K^P |\mathbf{Q}| \mathbf{s}^H \mathbf{Q}^{-1} \mathbf{g} \end{aligned} \quad (\text{B.3})$$

It is clear that the solution to (B.3) for α is the same as the one for the MLED case in (17) but directly adapted to the SDS detection scenario

$$\hat{\alpha} = \frac{\mathbf{s}^H \mathbf{Q}^{-1} \mathbf{g}}{\mathbf{s}^H \mathbf{Q}^{-1} \mathbf{s}} \quad (\text{B.4})$$

When this solution (B.4) is plugged into (B.2), the resulting equation is the same as (24). When there is no target in the radar detection scenario, the amplitude of the returned waveform is $\alpha = 0$. Plugging this into (B.2) results in Eq. (25).

Appendix C. Proof of Lindeberg's condition for the multistatic MLED approximation

In terms of the notation used in this paper, Lindeberg's condition takes the following form:

$$\lim_{MN \rightarrow \infty} \frac{1}{\sigma_M^2} \sum_{k=0}^{MN} \int_{|T_{M(k)} - \mu_{M(k)}| > \epsilon \sigma_M} (T_{M(k)} - \mu_{M(k)})^2 f_k(T_{M(k)}) dT_{M(k)} = 0 \quad (\text{C.1})$$

where the subscript (m, n) indicating the path between the m th transmitter and the n th receiver has been replaced with the generic subscript k for convenience. The term $T_{M(k)}$ represents the k th component in the sum (21). The probability density function $f_k(T_{M(k)})$ is associated with the bistatic MLED random variable (28). If (C.1) holds for any constant $\epsilon > 0$, then the condition is sufficient to claim that the multistatic MLED random variable (31) will converge to a Gaussian distribution as the number of transmit–receive pairs $M \times N$ goes to infinity. Chebyshev's inequality for the variance of the bistatic MLED detector states that

$$P\left(\left|T_{M(k)} - \mu_{M(k)}\right| \geq \epsilon \sigma_M\right) \leq \frac{\sigma_{M(k)}^2}{\epsilon^2 \sigma_M^2} \quad (\text{C.2})$$

Note that the mean $\mu_{M(k)}$ given in (42) and the variance $\sigma_{M(k)}^2$ from (43), considering a realistic system with finite time samples K and receive sensors P , both exist and are finite. This is due to the assumption that $\lambda_{m,n}$ is finite because the SNR $\rho_{m,n}$ is practically finite. The term σ_M^2 can be written in the form

$$\sigma_M^2 = \sum_{m,n} a_{m,n} \lambda_{m,n}^2 + \sum_{m,n} b_{m,n} \lambda_{m,n} + cMN \quad (\text{C.3})$$

where $a_{m,n}, b_{m,n}, c \in \mathbb{R}$. The sum in (C.3) goes to infinity as $M \times N \rightarrow \infty$. Therefore, the right-hand side of Chebyshev's inequality (C.2) goes to 0 since $\epsilon \neq 0$ is a constant. Therefore the left-hand side probability in the inequality is bounded by 0, which translates to

$$\lim_{M \times N \rightarrow \infty} \int_{|T_{M(k)} - \mu_{M(k)}| > \epsilon \sigma_M} f_k(T_{M(k)}) dT_{M(k)} = 0 \quad (\text{C.4})$$

Combined with the fact that the mean $\mu_{M(k)}$ is finite, this proves that each term in the sum (C.1) converges to 0 in the limit. Therefore the whole sum converges to 0 and Lindeberg's condition is satisfied, which justifies the Gaussian approximation of the multistatic MLED threshold detector.

Appendix D. Proof of Lindeberg's condition for the multistatic GMLED approximation

The expectation and second moment of the bistatic GMLED threshold detector given in (53) and (55) respectively are finite due to the assumptions that the parameters K, P , and $\lambda_{m,n}$ are practically finite (see Appendix C). In this proof the following logarithmic inequality will be used:

$$\log x \leq x - 1 \quad (\text{D.1})$$

From (D.1) an upper bound for the expectation of the logarithm of the bistatic GMLED threshold detector can be obtained

$$E[\log T_{G(m,n)}] \leq E[T_{G(m,n)} - 1] \quad (\text{D.2})$$

where the right-hand side of (D.2) is finite. Moreover, due to the nature of the random variables involved, it can be concluded that the expectation in the same equation is bounded from below by the case when the non-centrality parameter of the F -distribution becomes zero, or $\lambda_{m,n} = 0$

$$\frac{1}{L} \leq E[\log T_{G(m,n)}] \quad (\text{D.3})$$

where the left-hand side of (D.2) is obtained from the expectation in (62). In a similar manner boundaries for the second moment of the logarithm of the bistatic GMLED threshold detector can be derived:

$$\frac{1}{L^2} \leq E[(\log T_{G(m,n)})^2] \leq E[(T_{G(m,n)} - 1)^2] \quad (\text{D.4})$$

The upper boundary in (D.4) comes from (D.1), while the lower one is derived from the fact that $E[x^2] \geq E[x]^2$. Combining (D.3), (D.2), and (D.4), it can be concluded that the variance of the logarithm of the bistatic GMLED detector is also bounded from below and above by certain finite bounds. The exact values of these bounds are not essential for the current proof and will therefore not be

calculated

$$\sigma_{lb}^2 \leq \sigma_{G(m,n)}^2 \leq \sigma_{ub}^2 \quad (D.5)$$

The bounds in (D.5) are enough to conclude that for any arbitrary constant $\epsilon > 0$

$$\lim_{M \times N \rightarrow \infty} \frac{\sigma_{G(m,n)}^2}{\epsilon^2 \sigma_G^2} = 0 \quad (D.6)$$

since the lower bounds on the total multistatic variance σ_G^2 tend to infinity as the number of transmitter–receiver pairs in the system tends to infinity. At this point the analogical Chebyshev bound to (C.2) for the GMLED becomes zero which, similar to Appendix C, proves the validity of Lindeberg's condition.

Appendix E. Supplementary data

Supplementary data associated with this paper can be found in the online version at <http://dx.doi.org/10.1016/j.sigpro.2015.04.001>.

References

- [1] D. Bliss, K. Forsythe, Multiple-input multiple-output (MIMO) radar and imaging: degrees of freedom and resolution, in: Conference Record of the Thirty-Seventh Asilomar Conference on Signals, Systems and Computers, vol. 1, 2003, pp. 54–59. <http://dx.doi.org/10.1109/ACSSC.2003.1291865>.
- [2] E. Fishler, A. Haimovich, R. Blum, D. Chizhik, L. Cimini, R. Valenzuela, MIMO radar: an idea whose time has come, in: Radar Conference, Proceedings of the IEEE, 2004, pp. 71–78. <http://dx.doi.org/10.1109/NRC.2004.1316398>.
- [3] E. Fishler, A. Haimovich, R. Blum, R. Cimini, D. Chizhik, R. Valenzuela, Performance of MIMO radar systems: advantages of angular diversity, in: Conference Record of the Thirty-Eighth Asilomar Conference on Signals, Systems and Computers, vol. 1, 2004, pp. 305–309. <http://dx.doi.org/10.1109/ACSSC.2004.1399142>.
- [4] E. Fishler, A. Haimovich, R. Blum, L.J. Cimini, D. Chizhik, R. Valenzuela, Spatial diversity in radars—models and detection performance, IEEE Trans. Signal Process. 54 (3) (2006) 823–838. <http://dx.doi.org/10.1109/TSP.2005.862813>.
- [5] N. Goodman, D. Bruyere, Optimum and decentralized detection for multistatic airborne radar, IEEE Trans. Aerosp. Electron. Syst. 43 (2) (2007) 806–813. <http://dx.doi.org/10.1109/TAES.2007.4285374>.
- [6] A. Haimovich, R. Blum, L. Cimini, MIMO radar with widely separated antennas, IEEE Signal Process. Mag. 25 (1) (2008) 116–129. <http://dx.doi.org/10.1109/MSP.2008.4408448>.
- [7] H. Godrich, A. Haimovich, R. Blum, Target localization accuracy gain in MIMO radar-based systems, IEEE Trans. Inf. Theory 56 (6) (2010) 2783–2803. <http://dx.doi.org/10.1109/TIT.2010.2046246>.
- [8] B. Shtarkalev, B. Mulgrew, Multistatic single data set target detection in unknown coloured Gaussian interference, in: Radar Conference (RADAR), 2013 IEEE, 2013, pp. 1–5. <http://dx.doi.org/10.1109/RADAR.2013.6585997>.
- [9] Y. Abramovich, G.J. Frazer, Bounds on the volume and height distributions for the MIMO radar ambiguity function, IEEE Signal Process. Lett. 15 (2008) 505–508. <http://dx.doi.org/10.1109/LSP.2008.922514>.
- [10] G. Frazer, Y. Abramovich, B. Johnson, MIMO radar limitations in clutter, in: Radar Conference, IEEE, 2009, pp. 1–5. <http://dx.doi.org/10.1109/RADAR.2009.4976946>.
- [11] R. Adve, T. Hale, M. Wicks, Practical joint domain localised adaptive processing in homogeneous and nonhomogeneous environments. 2. Nonhomogeneous environments, IEE Proc. Radar Sonar Navig. 147 (2) (2000) 66–74. <http://dx.doi.org/10.1049/ip-rsn:20000085>.
- [12] E. Aboutanios, B. Mulgrew, A STAP algorithm for radar target detection in heterogeneous environments, in: IEEE/SP 13th Workshop on Statistical Signal Processing, 2005, pp. 966–971. <http://dx.doi.org/10.1109/SSP.2005.1628734>.
- [13] C.-H. Lim, B. Mulgrew, E. Aboutanios, Bistatic JDL-STAP for ground moving target detection, in: IET International Conference on Radar Systems, 2007, pp. 1–5.
- [14] C.-H. Lim, Bistatic space–time adaptive processing for ground moving target indication (Ph.D. thesis), Engineering, The University of Edinburgh, URL: <http://hdl.handle.net/1842/6373>, October 2006.
- [15] C. Lim, E. Aboutanios, B. Mulgrew, Training strategies for joint domain localised-space–time adaptive processing in a bistatic environment, IEE Proc. Radar Sonar Navig. 153 (6) (2006) 516–524. <http://dx.doi.org/10.1049/ip-rsn:20050121>.
- [16] E. Aboutanios, B. Mulgrew, Hybrid detection approach for STAP in heterogeneous clutter, IEEE Trans. Aerosp. Electron. Syst. 46 (3) (2010) 1021–1033. <http://dx.doi.org/10.1109/TAES.2010.5545171>.
- [17] P. Wang, H. Li, B. Himed, A new parametric GLRT for multichannel adaptive signal detection, IEEE Trans. Signal Process. 58 (1) (2010) 317–325. <http://dx.doi.org/10.1109/TSP.2009.2030835>.
- [18] P. Wang, H. Li, B. Himed, Moving target detection using distributed MIMO radar in clutter with nonhomogeneous power, IEEE Trans. Signal Process. 59 (10) (2011) 4809–4820. <http://dx.doi.org/10.1109/TSP.2011.2160861>.
- [19] P. Wang, H. Li, B. Himed, Parametric Rao tests for multichannel adaptive detection in partially homogeneous environment, IEEE Trans. Aerosp. Electron. Syst. 47 (3) (2011) 1850–1862. <http://dx.doi.org/10.1109/TAES.2011.5937269>.
- [20] P. Wang, H. Li, B. Himed, A parametric moving target detector for distributed MIMO radar in non-homogeneous environment, IEEE Trans. Signal Process. 61 (9) (2013) 2282–2294. <http://dx.doi.org/10.1109/TSP.2013.2245323>.
- [21] J.-F. Degurse, S. Marcos, L. Savy, Subspace-based and single dataset methods for STAP in heterogeneous environments, in: IET International Conference on Radar Systems (Radar 2012), 2012, pp. 1–6. <http://dx.doi.org/10.1049/cp.2012.1693>.
- [22] J.-F. Degurse, L. Savy, S. Marcos, J.-P. Molinié, Deterministic aided STAP for target detection in heterogeneous situations, vol. 2013, 2013, p. 10. URL: <http://dx.doi.org/10.1155/2013/826935>.
- [23] D. Bruyere, N. Goodman, Adaptive detection and diversity order in multistatic radar, IEEE Trans. Aerosp. Electron. Syst. 44 (4) (2008) 1615–1623. <http://dx.doi.org/10.1109/TAES.2008.4667736>.
- [24] C.Y. Chong, F. Pascal, J. Ovarlez, M. Lesturgie, MIMO radar detection in non-Gaussian and heterogeneous clutter, IEEE J. Sel. Top. Signal Process. 4 (1) (2010) 115–126. <http://dx.doi.org/10.1109/JSTSP.2009.2038980>.
- [25] L. Kong, M. Yang, B. Zhao, Adaptive detection for shared-spectrum multistatic radar in Gaussian clutter, in: Radar Conference (RADAR), 2012 IEEE, 2012, pp. 0309–0313. <http://dx.doi.org/10.1109/RADAR.2012.6212156>.
- [26] J. Liu, Z.-J. Zhang, Y. Cao, S. Yang, A closed-form expression for false alarm rate of adaptive MIMO-GLRT detector with distributed MIMO radar, Signal Process. 93 (9) (2013) 2771–2776. <http://dx.doi.org/10.1016/j.sigpro.2013.03.001> URL: <http://www.sciencedirect.com/science/article/pii/S0165168413000753>.
- [27] W. Melvin, A STAP overview, IEEE Aerosp. Electron. Syst. Mag. 19 (1) (2004) 19–35. <http://dx.doi.org/10.1109/MAES.2004.1263229>.
- [28] R. Ash, C. Doléans-Dade, Probability and Measure Theory, Harcourt/Academic Press, Burlington, MA, 2000 URL: <http://books.google.co.uk/books?id=GkqQoRcO2QC>.
- [29] D. Bliss, K. Forsythe, S. Davis, G. Fawcett, D. Rabideau, L. Horowitz, S. Kraut, GMTI MIMO radar, in: Waveform Diversity and Design Conference, International, 2009, pp. 118–122. <http://dx.doi.org/10.1109/WDDC.2009.4800327>.
- [30] J. Kantor, D. Bliss, Clutter covariance matrices for GMTI MIMO radar, in: Conference Record of the Forty Fourth Asilomar Conference on Signals, Systems and Computers (ASILOMAR), 2010, pp. 1821–1826. <http://dx.doi.org/10.1109/ACSSC.2010.5757856>.
- [31] J. Ward, Space–time Adaptive Processing for Airborne Radar, Technical Report, MIT Lincoln Labs, December 1994. URL: <http://handle.dtic.mil/100.2/ADA293032>.
- [32] B. Shtarkalev, B. Mulgrew, Effects of FDMA/TDMA orthogonality on the Gaussian pulse train MIMO ambiguity function, IEEE Signal Process. Lett. 22 (2) (2015) 153–157. <http://dx.doi.org/10.1109/LSP.2014.2351256>.
- [33] W. Melvin, R. Hancock, M. Rangaswamy, J. Parker, Adaptive distributed radar, in: Radar Conference – Surveillance for a Safer World, 2009, RADAR, International, 2009, pp. 1–6.
- [34] L. Brennan, L. Reed, Theory of adaptive radar, IEEE Trans. Aerosp. Electron. Syst. AES-9 (2) (1973) 237–252. <http://dx.doi.org/10.1109/TAES.1973.309792>.
- [35] P. Stoica, H. Li, J. Li, A new derivation of the APES filter, IEEE Signal Process. Lett. 6 (8) (1999) 205–206. <http://dx.doi.org/10.1109/97.74866>.

- [36] F. Robey, D. Fuhrmann, E. Kelly, R. Nitzberg, A CFAR adaptive matched filter detector, *IEEE Trans. Aerosp. Electron. Syst.* 28 (1) (1992) 208–216, <http://dx.doi.org/10.1109/7.135446>.
- [37] E. Kelly, An adaptive detection algorithm, *IEEE Trans. Aerosp. Electron. Syst.* AES-22 (2) (1986) 115–127, <http://dx.doi.org/10.1109/TAES.1986.310745>.
- [38] A. Robinson, B. Mulgrew, A comparison of contemporary space–time adaptive processing techniques for GMTI, in: *IET International Conference on Radar Systems (Radar 2012)*, 2012, pp. 1–5. <http://dx.doi.org/10.1049/cp.2012.1691>.
- [39] F. Frishman, On the arithmetic means and variances of products and ratios of random variables, in: G. Patil, S. Kotz, J. Ord (Eds.), *Statistical Distributions in Scientific Work*, vol. 1, D. Reidel Publishing Company, Dordrecht–Holland, 1975, pp. 401–406.
- [40] P. Patnaik, The non-central χ^2 and F-distributions and their applications, *Biometrika* 36 (1–2) (1949) 202–232.
- [41] N.J. Willis, *Bistatic Radar*, 2nd ed. SciTech Publishing, Raleigh, NC, 2005 URL: (<http://books.google.co.uk/books?id=U0XG5WB-vY8C>).
- [42] G.W. Stimson, *Introduction to Airborne Radar*, 2nd ed. SciTech Publishing, Inc., Raleigh, NC, 1998.
- [43] G. Mhlbach, M. Gasca, A generalization of Sylvester's identity on determinants and some applications, *Linear Algebra Appl.* 66 (1985) 221–234. [http://dx.doi.org/10.1016/0024-3795\(85\)90134-X](http://dx.doi.org/10.1016/0024-3795(85)90134-X) URL: (<http://www.sciencedirect.com/science/article/pii/002437958590134X>).